Формирование градиентной структуры в метастабильной аустенитной стали для улучшения комплекса механических свойств

Докладчик – Панов Дмитрий Олегович,
старший научный сотрудник Лаборатории объемных наноструктурных материалов НИУ БелГУ,
к.т.н., доцент

Contents

1. Motivation

D. Panov, A. Pertsev, A. Smirnov, V. Khotinov, Y. Simonov, Metastable austenitic steel structure and mechanical properties evolution in the process of cold radial forging, Materials 12 (2019) 2058

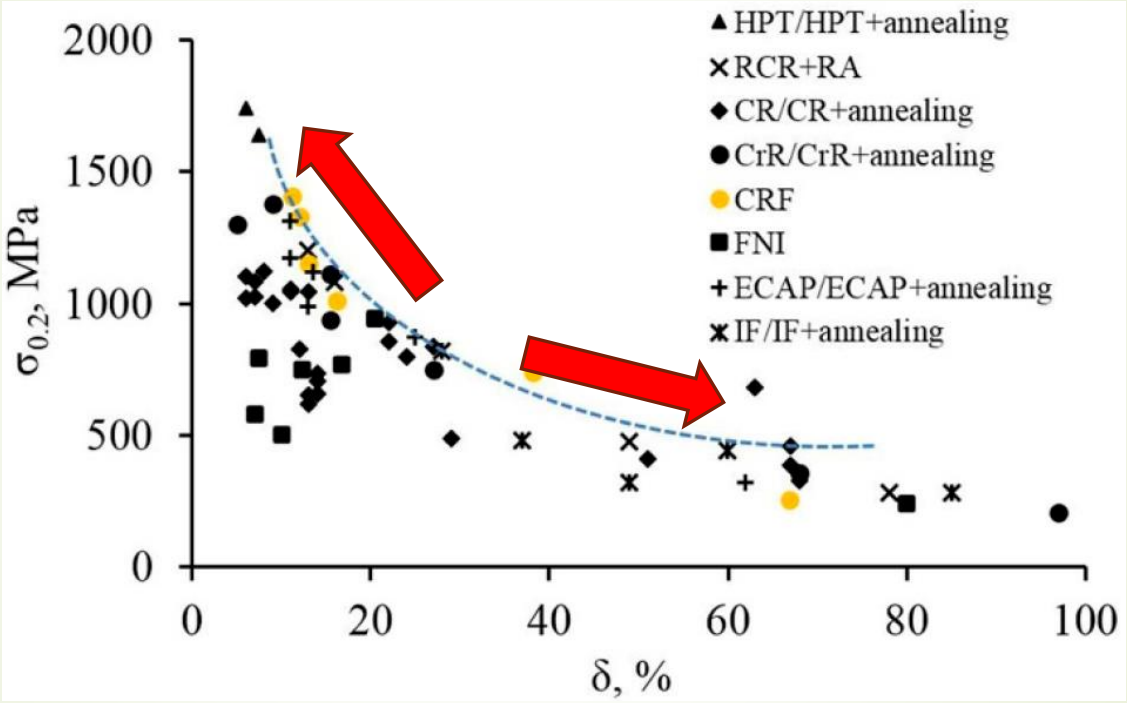

Figure. Yield strength—elongation to fracture relation of the 321 MASS after different strengthening treatment methods. Note: high pressure torsion (HPT), repetitive cold rolling and reversion annealing (RCR + RA), cold rolling (CR), cryogenic rolling (CrR), cold radial forging (CRF), fast neutron irradiation (FNI), equal channel angular pressing (ECAP), isothermal forging (IF).

1. Motivation

X. Wu et al. Extraordinary strain hardening by gradient structure // PNAS, 2014 vol. 111, no. 20, 7197–7201.

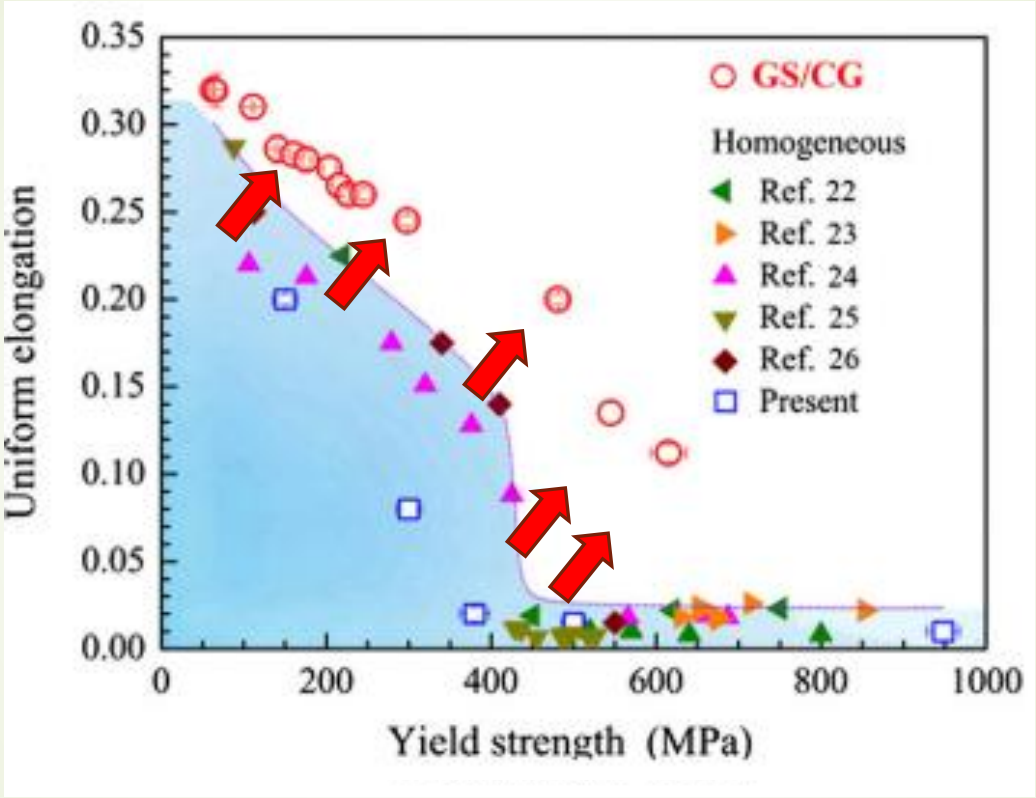

Figure. Superior mechanical property. Strength and ductility in the GS–CG samples of IF-steel compared with their homogeneous counterparts.

1. Motivation

W.L. Li et al. Fabrication of a gradient nano-micro-structured surface layer on bulk copper by means of a surface mechanical grinding treatment, Scripta Materialia, Volume 59, Issue 5, 2008, Pages 546-549.

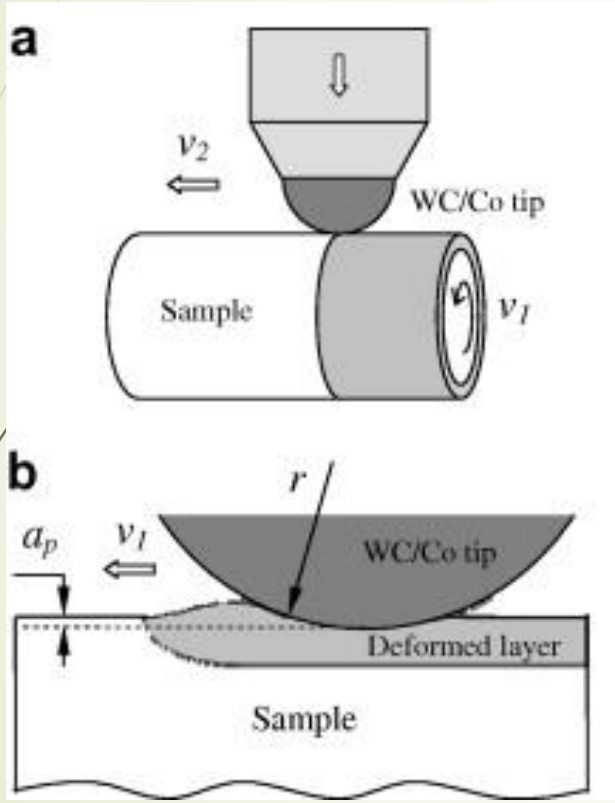

Figure. Schematic illustrations of (a) the surface mechanical grinding treatment (SMGT) set-up and (b) the plastic deformation layer induced by the tool tip.

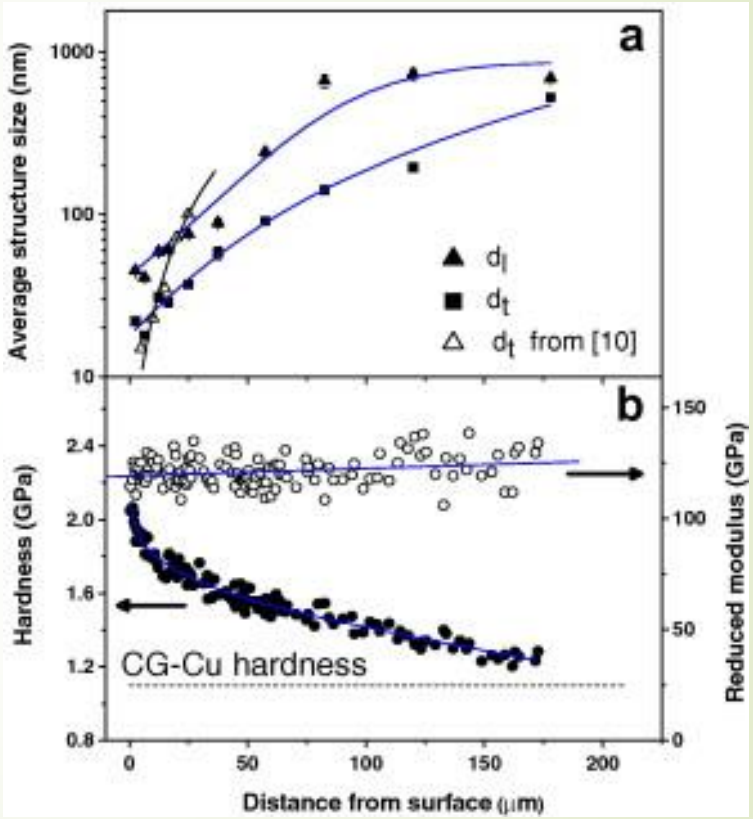

Figure. Variations of (a) the average structure size and (b) hardness and reduced modulus with distance from treated surface.

1. Motivation

T. H. Fang et al. Revealing Extraordinary Intrinsic Tensile Plasticity in Gradient Nano-Grained Copper. Science. 331, 1587 (2011).

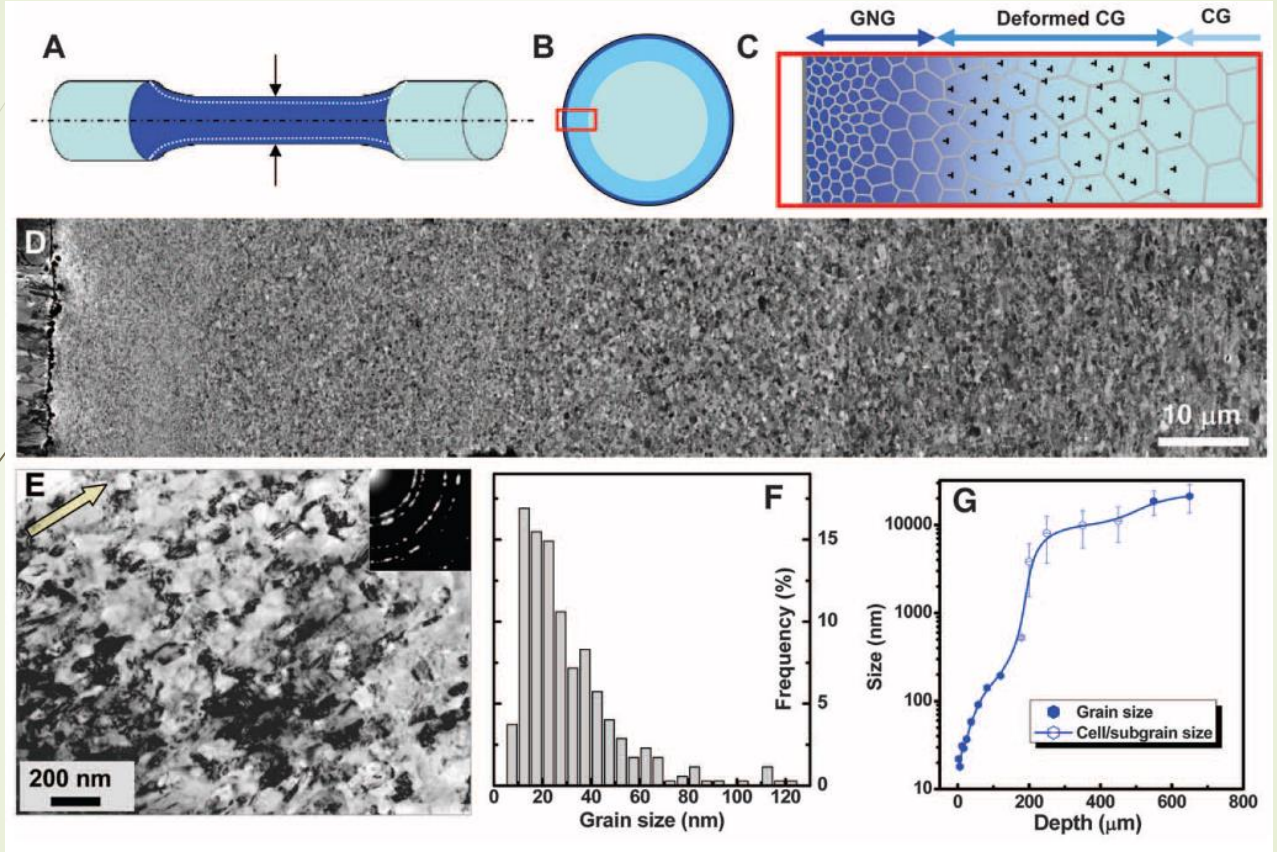

Figure. (A) Schematic of the tensile bar sample of which the gauge section was processed by means of SMGT. (B and C) Schematic of the cross-sectional microstructure of the gauge consisting of a GNG layer (dark blue) and a deformed CG layer (blue) on a CG core (light blue). (D) A typical cross-sectional SEM image of a SMGT Cu sample. (E) A cross-sectional bright-field TEM image of microstructures 3 mmbelow the treated surface. The arrow indicates the processing direction, and the inset shows the electron diffraction pattern. (F) A transversal grain size distribution from TEM measurements in the top 5-mm-deep layer. (G) Variation of average transversal grain (subgrain or cell) sizes along depth from the surface. Error bars represent the standard deviation of grain-size measurements.

1. Motivation

T. H. Fang et al. Revealing Extraordinary Intrinsic Tensile Plasticity in Gradient Nano-Grained Copper. Science. 331, 1587 (2011).

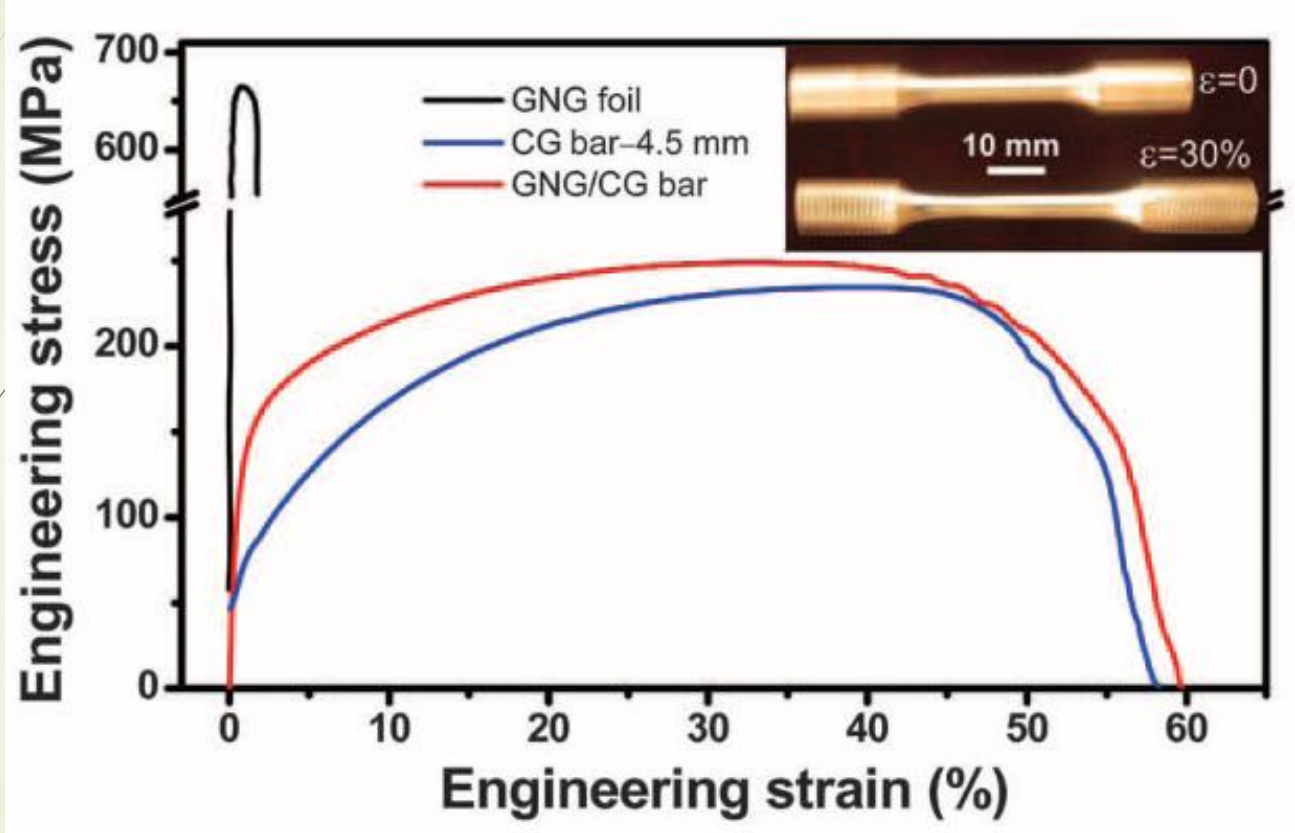

Figure. Quasi-static tensile engineering stress-strain curves for the CG Cu bar sample with a gauge diameter of 4.5 mm, the GNG/CG bar sample, and a free-standing GNG foil sample (the top 50-mm-thick layer was removed from the GNG/CG sample, gauge dimensions: 4 mm by 2 mm by 0.05 mm), respectively. Strain rate is 6 × 10−4 s−1. Inset shows the tensile GNG/CG bar samples before and after tension (with a nominal strain of 30%). (B)

1. Motivation

Zhi Zenga et al. Gradient plasticity in gradient nano-grained metals // Extreme Mechanics Letters 8 (2016) 213–219.

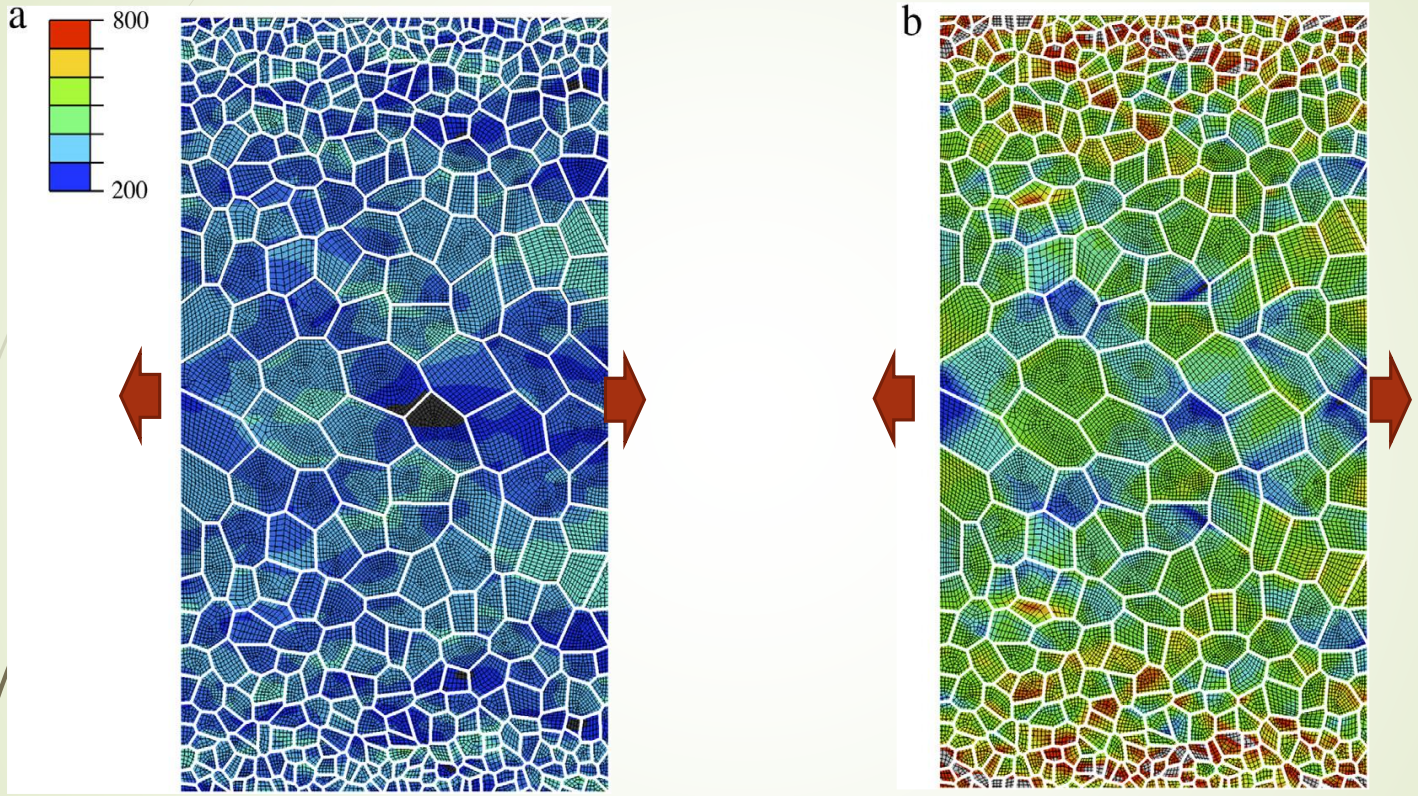

Figure. Contours of axial stresses at the applied strain load of (a) 0.2% and (b) 1%. The color map is in the unit of MPa.

1. Motivation

Zhi Zenga et al. Gradient plasticity in gradient nano-grained metals // Extreme Mechanics Letters 8 (2016) 213–219.

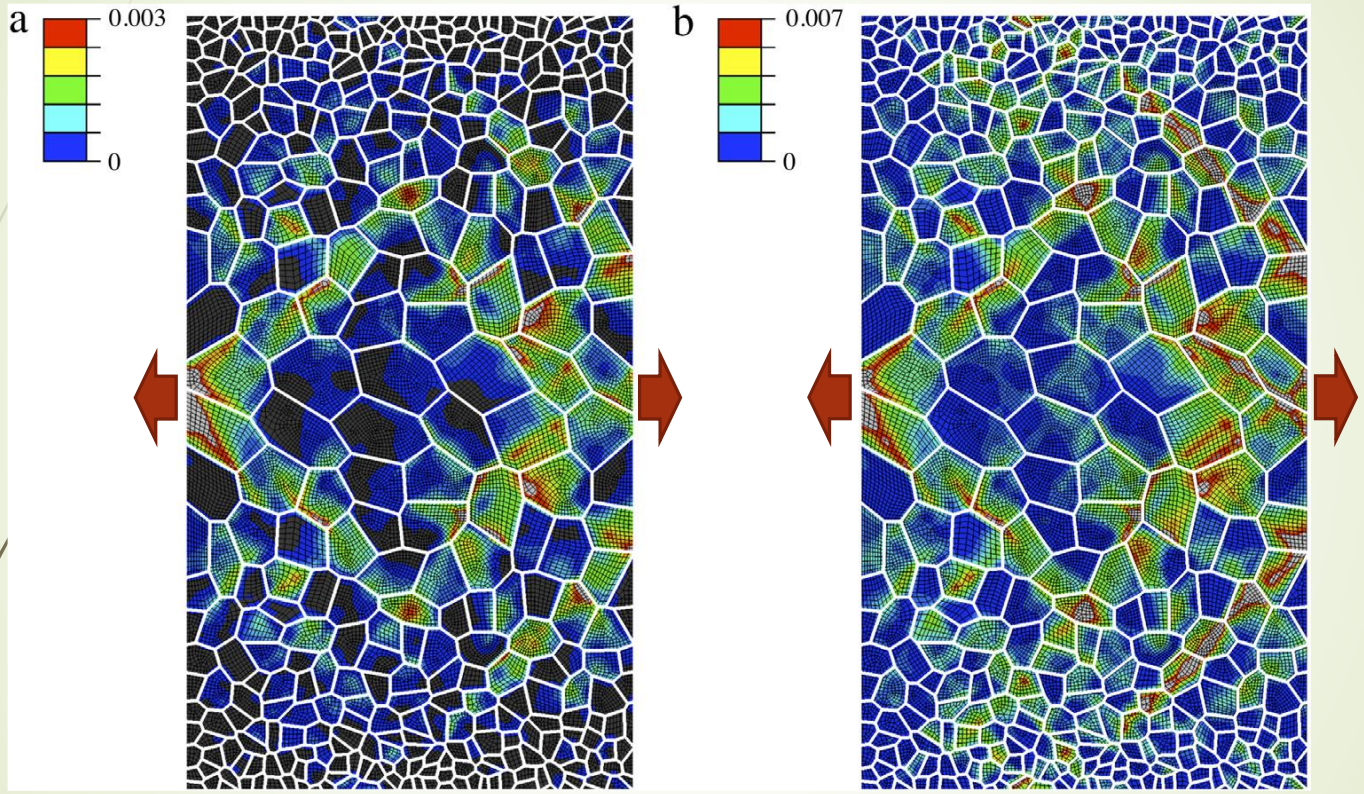

Figure. Contours of axial plastic strains at the applied strain load of (a) 0.33% and (b) 0.5%.

2. Experimental procedures.

The program material:
AISI 321-type steel (wt.%: C-0.07, Cr-18.75, Ni-9.20, Ti-0.59, Mn-1.12, Si-0.39, S-0.005, P-0.019, and Fe balance).

Applied methods:

- transitions electron microscopy (a JEOL JEM-2100 electron microscope);
- Vickers hardness examination (a Wolpert 402MVD semi-automatic hardness tester);
- eddy current testing (a FERRITSCOPE FMP30 apparatus);
- tensile testing (an Instron 5882 electromechanical testing system);
- notch toughness testing (an Instron SI-1 M Charpy impact testing machine);
- fractography (a FEI Nova NanoSEM 450 scanning electron microscope).

3. The principle of deformation processing.

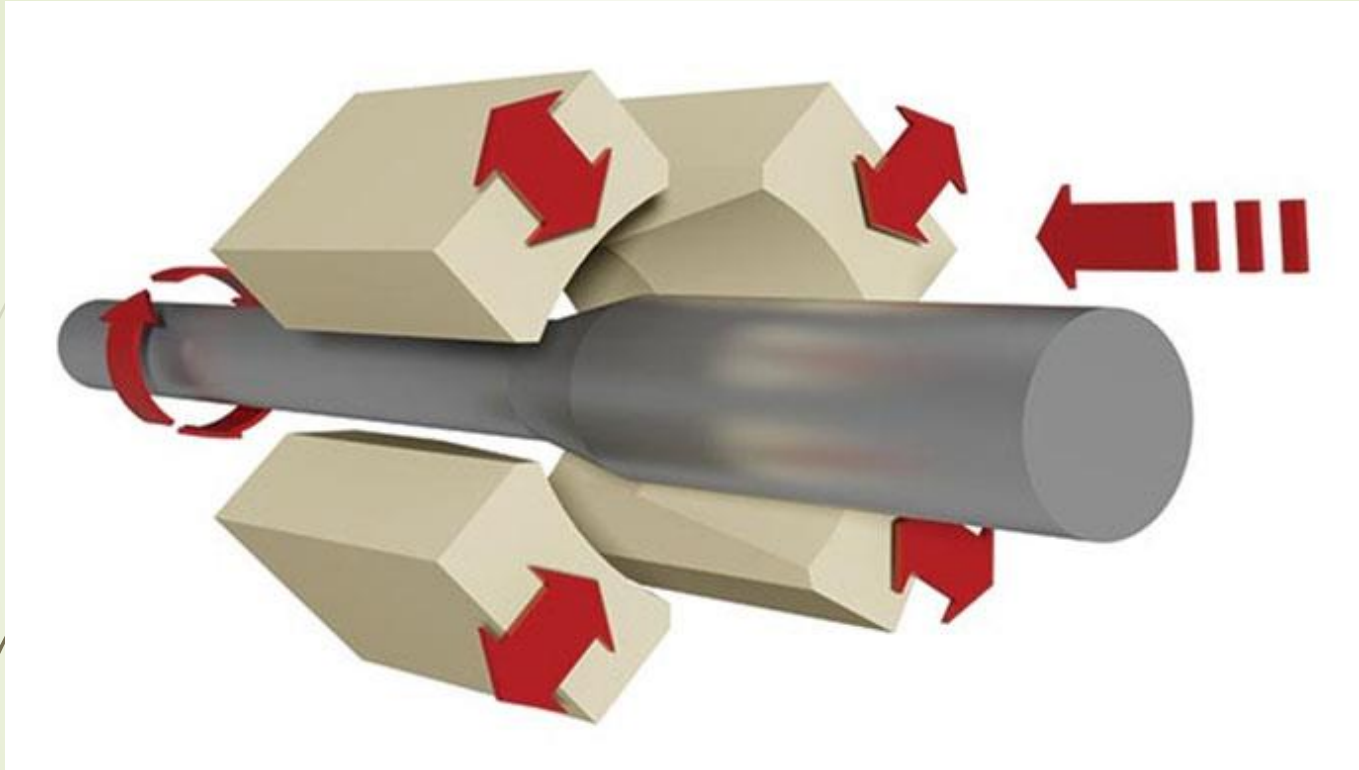

Figure. The principle of swaging [https://www.forgemag.com/articles/84977-shaping-future-innovations-with-radial-forging].

4. Choice of annealing parameters.

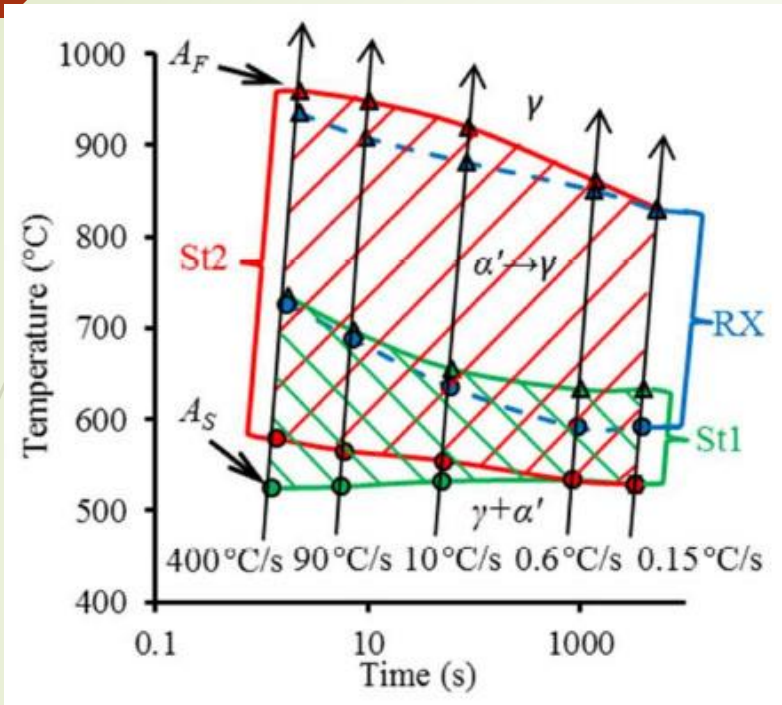

Figure. The reversion-temperature-time diagram for the as-processed program steel. Notation: St1—first reversion stage; St2—second reversion stage; RX—recrystallization [1].

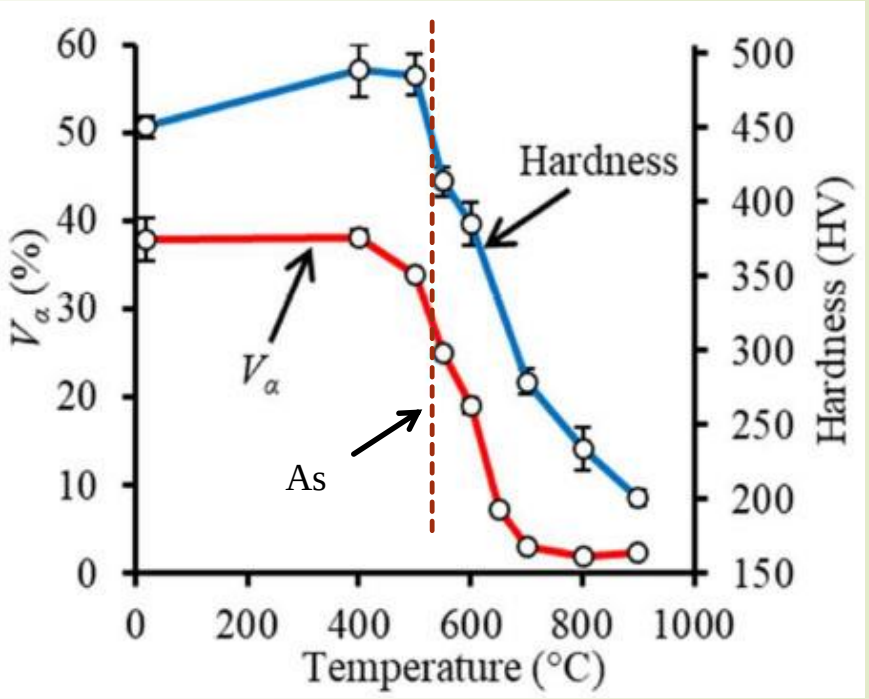

Figure. Effect of annealing temperature on the α-phase content (Vα, %) and hardness [1].

[1] D. Panov, E. Kudryavtsev, R. Chernichenko, A. Smirnov, N. Stepanov, Y. Simonov, S. Zherebtsov, G. Salishchev, Mechanisms of the reverse martensite-to-austenite transformation in a metastable austenitic stainless steel, Metals (Basel) 11 (2021) 1–13.

5. Mechanical properties.

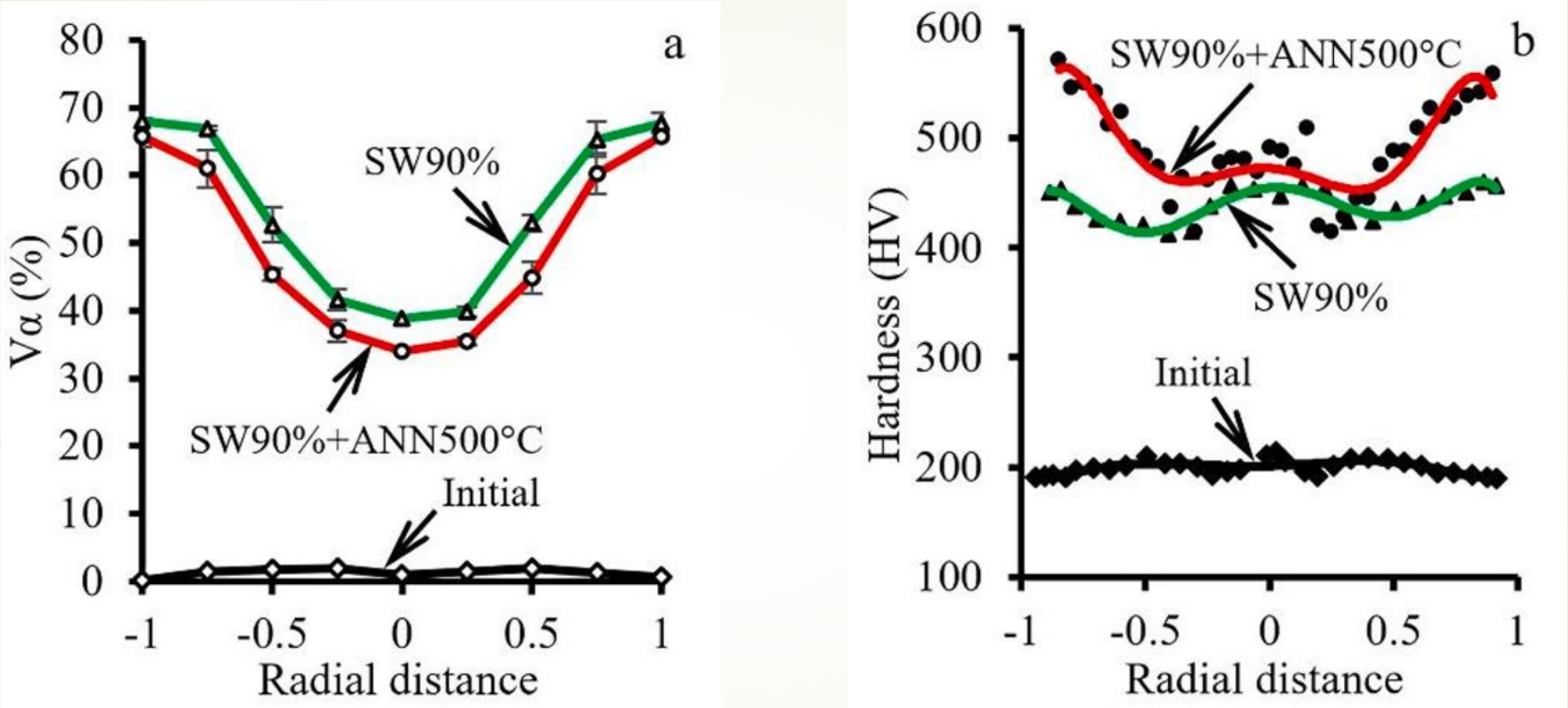

Figure. Distributions of (a) α-phase and (b) microhardness along the section of the bar after different treatment modes [1].

[1] Panov, D.O.; Chernichenko, R.S.; Naumov, S.V.; Pertcev, A.S.; Stepanov, N.D.; Zherebtsov, S.V.; Salishchev, G.A. Excellent strength-toughness synergy in metastable austenitic stainless steel due to gradient structure formation. Mater. Lett. 2021, 303, 130585.

6. Structure characterization.

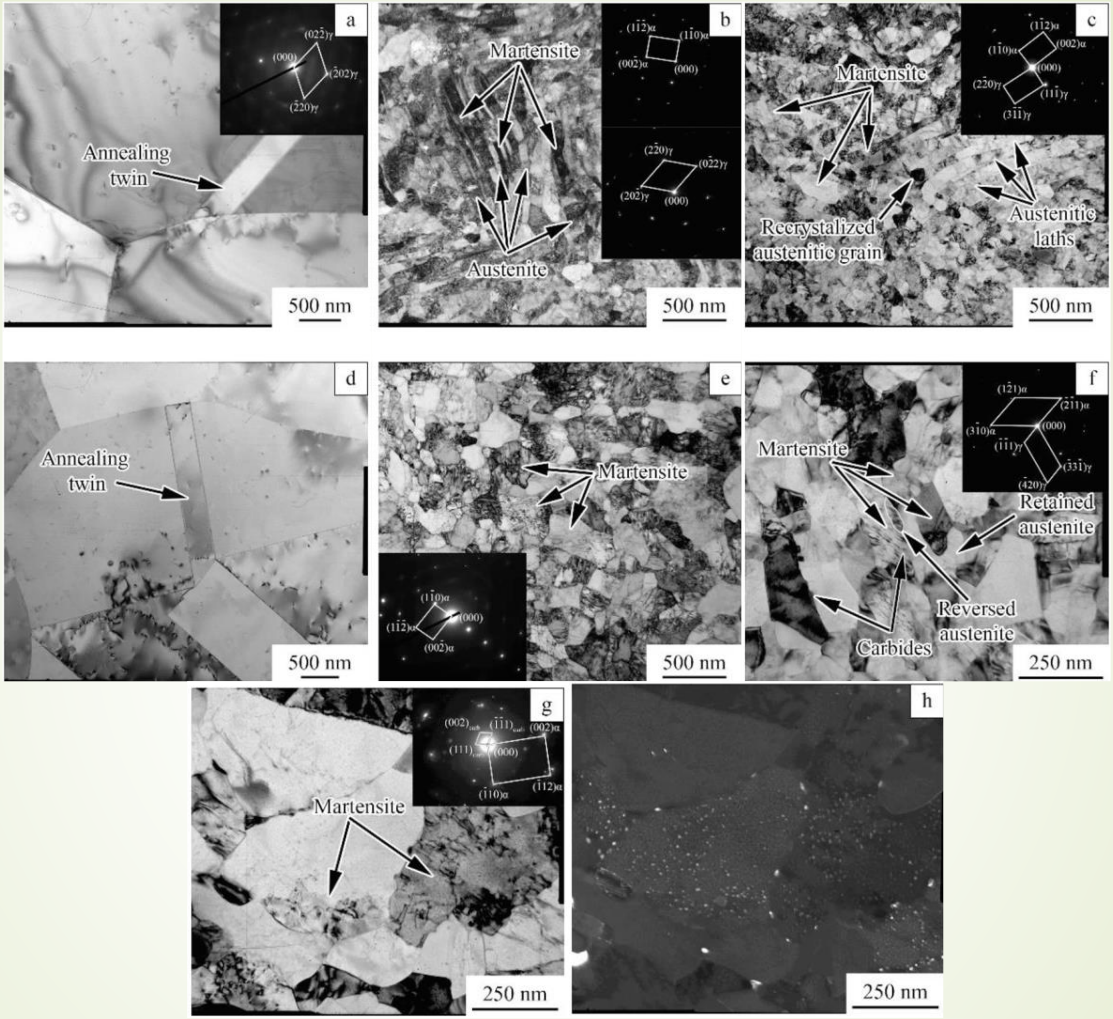

Figure. TEM micrographs of (a), (d) the initial condition; (b), (e) the swaged bar; (c), (f), (g), (h) swaged and annealed at 500 ◦C condition; (a)–(c) center and (d)–(h) edge of the bar. (h) is dark field in (222)carb reflection of a Me23C6-type carbide from (g). Note higher magnification in (f)–(h) [1] .

[1] Panov, D.O.; Chernichenko, R.S.; Naumov, S.V.; Pertcev, A.S.; Stepanov, N.D.; Zherebtsov, S.V.; Salishchev, G.A. Excellent strength-toughness synergy in metastable austenitic stainless steel due to gradient structure formation. Mater. Lett. 2021, 303, 130585.

7. Estimation of Orowan strengthening.

Orowan strengthening was evaluated using the following equation [1]:

$$\Delta\sigma_{YOS} = M\frac{0.4Gb}{\pi\lambda}\frac{\ln(2r/b)}{\sqrt{1-\upsilon}} \approx 358\text{MPa},$$

where G is the matrix shear modulus; b = 0.248 nm is the Burgers vector; υ = 0.3 is the matrix Poisson's ratio; λ is interparticle spacing; M = 2.9 is the Taylor factor for the bcc polycrystalline matrix; r = 3 nm and f = 0.004 is the average particles radius and volume fraction, respectively. Taking into consideration the volume fraction of strengthened phase, an increase in strength at the center and edge was ~120MPa and ~240MPa, respectively.

References

[1] H. Wen, T.D. Topping, D. Isheim, D.N. Seidman, E.J. Lavernia, Strengthening mechanisms in a high-strength bulk nanostructured Cu-Zn-Al alloy processed via cryomilling and spark plasma sintering, Acta Mater. 61 (2013) 2769–2782. https://doi.org/10.1016/j.actamat.2012.09.036.

8. Mechanical properties.

Table. Mechanical properties of the 321-type steel [1].

Condition	YS, MPa	UTS, MPa	δ, %	Notch toughness, MJ/m^2
Initial	155	610	83.2	1.58
Swaging 90%	1405	1410	11.2	0.70
Swaging 90% + annealing 500 °C	1490	1550	9.5	1.42

[1] Panov, D.O.; Chernichenko, R.S.; Naumov, S.V.; Pertcev, A.S.; Stepanov, N.D.; Zherebtsov, S.V.; Salishchev, G.A. Excellent strength-toughness synergy in metastable austenitic stainless steel due to gradient structure formation. Mater. Lett. 2021, 303, 130585.

8. Fracture analysis.

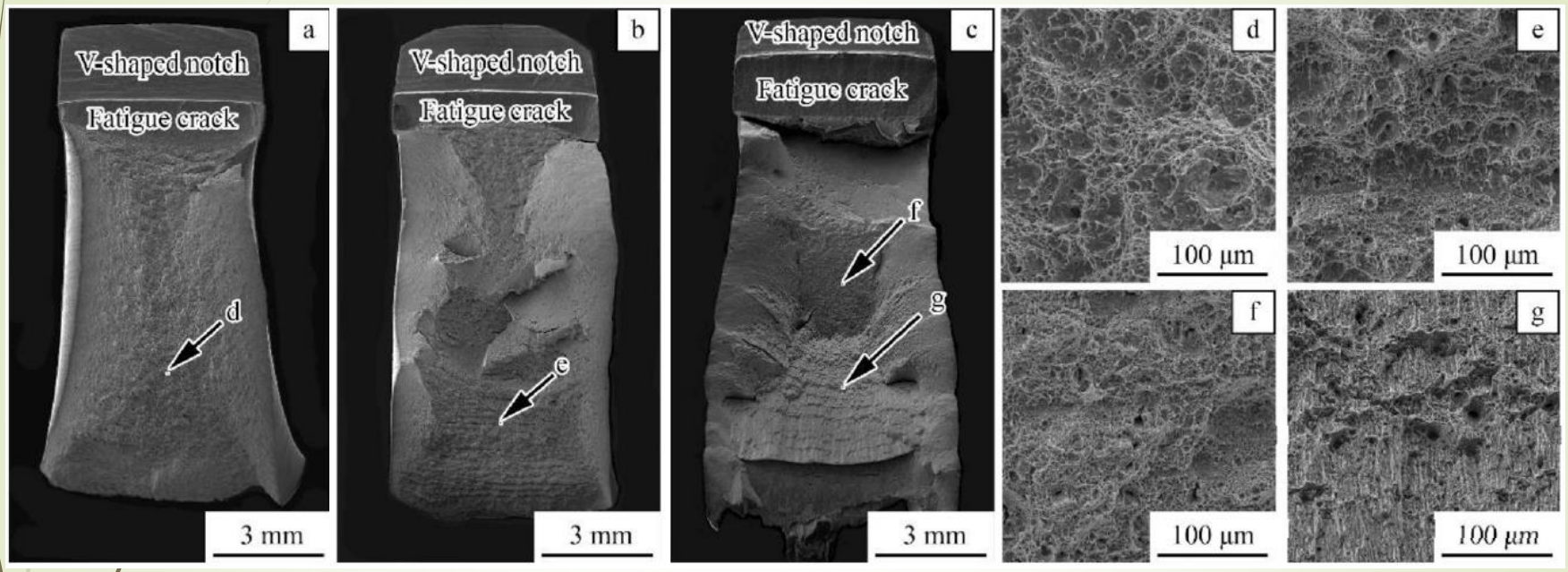

Figure. (a)–(c) SEM-overviews of fracture surfaces and (d)–(g) SEM-micrographs of the fracture surfaces of the program steel in: (a), (d) – initial condition; (b), (e) – swaged condition, (c), (f), (g) – after annealing at 500 °C [1].

[1] Panov, D.O.; Chernichenko, R.S.; Naumov, S.V.; Pertcev, A.S.; Stepanov, N.D.; Zherebtsov, S.V.; Salishchev, G.A. Excellent strength-toughness synergy in metastable austenitic stainless steel due to gradient structure formation. Mater. Lett. 2021, 303, 130585.

10. Conclusions [1]

In summary, the current study revealed the effect of cold swaging and subsequent annealing at 500 ◦C on the structure and mechanical properties of the AISI 321-type metastable austenitic stainless steel. Cold swaging to 90% of strain resulted in a noticeable variation in morphology and phase composition from the center to edge. After annealing at 500 °C, microstructure refinement due to the onset of recrystallization and reverse martensite-to-austenite transformation was detected. A significant strengthening was observed after annealing. Meanwhile, notch toughness of the annealed condition almost reached the level of the initial condition.

Funding: This research was funded by the Russian Science Foundation Grant no. 20-79-10094.

[1] Panov, D.O.; Chernichenko, R.S.; Naumov, S.V.; Pertcev, A.S.; Stepanov, N.D.; Zherebtsov, S.V.; Salishchev, G.A. Excellent strength-toughness synergy in metastable austenitic stainless steel due to gradient structure formation. Mater. Lett. 2021, 303, 130585.

11. Публикации авторов по теме

1. Panov, D.O.; Chernichenko, R.S.; Naumov, S.V.; Pertcev, A.S.; Stepanov, N.D.; Zherebtsov, S.V.; Salishchev, G.A. Excellent strength-toughness synergy in metastable austenitic stainless steel due to gradient structure formation. Mater. Lett. 2021, 303, 130585.
2. Panov, D.; Pertsev, A.; Smirnov, A.; Khotinov, V.; Simonov, Y. Metastable austenitic steel structure and mechanical properties evolution in the process of cold radial forging. Materials 2019, 12, 2058.
3. Panov, D.; Chernichenko, R.; Kudryavtsev, E.; Klimenko, D.; Naumov, S.; Pertcev, A. Effect of Cold Swaging on the Bulk Gradient Structure Formation and Mechanical Properties of a 316-Type Austenitic Stainless Steel. Materials 2022, 15, 2468.
4. Panov D., Kudryavtsev E., Chernichenko R., Smirnov A., Stepanov N., Simonov Y., Zherebtsov S., Salishchev G. Mechanisms of the reverse martensite-to-austenite transformation in a metastable austenitic stainless steel, Metals (Basel) 11 (2021) 1–13.

Thank you for your attention!